Neuropsychopharmacology (2017) 42, 963–973

www.neuropsychopharmacology.org

Haloperidol Selectively Remodels Striatal Indirect Pathway Circuits

Luke E Sebel[1], Steven M Graves[1], C Savio Chan[1] and D James Surmeier*[,1]

[1]*Department of Physiology, Feinberg School of Medicine, Northwestern University, Chicago, IL, USA*

Typical antipsychotic drugs are widely thought to alleviate the positive symptoms of schizophrenia by antagonizing dopamine D_2 receptors expressed by striatal spiny projection neurons (SPNs). What is less clear is why antipsychotics have a therapeutic latency of weeks. Using a combination of physiological and anatomical approaches in *ex vivo* brain slices from transgenic mice, it was found that 2 weeks of haloperidol treatment induced both intrinsic and synaptic adaptations specifically within indirect pathway SPNs (iSPNs). Perphenazine treatment had similar effects. Some of these adaptations were homeostatic, including a drop in intrinsic excitability and pruning of excitatory corticostriatal glutamatergic synapses. However, haloperidol treatment also led to strengthening of a subset of excitatory corticostriatal synapses. This slow remodeling of corticostriatal iSPN circuitry is likely to play a role in mediating the delayed therapeutic action of neuroleptics.
Neuropsychopharmacology (2017) **42,** 963–973; doi:10.1038/npp.2016.173; published online 12 October 2016

INTRODUCTION

Dopamine signaling in the basal ganglia assists in goal-directed action selection and habit formation by providing information about the outcome of goal-directed behavior and the motivational salience of stimuli (Redgrave *et al*, 2010; Winton-Brown *et al*, 2014). Dopamine fibers 'broadcast' this signal to all cell types within the striatum, but the major target of this innervation is the principal spiny projection neuron (SPN) (Gerfen and Surmeier, 2011). There are two main classes of SPNs. The so-called direct pathway SPNs (dSPNs) promote the selection of appropriate actions and indirect pathway SPNs (iSPNs) help suppress unwanted ones (Frank, 2011). Dopamine bidirectionally modulates the activity of these two classes of SPNs. This bidirectionality reflects the dichotomous expression of G protein-coupled DA receptors (GPCR) by these two SPN populations: dSPNs express D_1 receptors (D_1R) that enhance excitability and excitatory glutamatergic synaptic transmission, whereas iSPNs express D_2 receptors (D_2Rs) that diminish excitability and excitatory synaptic transmission.

Antipsychotic drugs antagonize dopamine D_2Rs at concentrations that correlate with their clinical potency (Creese *et al*, 1976; Seeman *et al*, 1976); however, their therapeutic benefits lag behind the acute blockade of D_2Rs by days, weeks, or even months (Agid *et al*, 2003; Leucht *et al*, 2005; Tauscher *et al*, 2002). Slow alterations in corticostriatal circuitry might underlie the time lag between neuroleptic treatment and effect (Konradi and Heckers, 2001). Animal studies investigating the chronic effects of the typical antipsychotic haloperidol have consistently demonstrated ultrastructural alterations in the striatum, including an increase in the number of perforated synapses (Meshul and Casey, 1989; Meshul *et al*, 1996; Roberts *et al*, 1995). In line with the anatomical data, chronic haloperidol was shown to cause an alteration in the induction of striatal synaptic plasticity in acute brain slices from rodents, biasing synaptic plasticity toward the potentiation of glutamatergic inputs on striatal neurons (Centonze *et al*, 2004). This site of action is consistent with studies implicating striatal glutamatergic signaling in the pathophysiology of schizophrenia (Laruelle *et al*, 2003).

Despite the plausibility of this hypothesis, the effect of chronic antipsychotic treatment on striatal physiology has not been examined systematically. Moreover, the anatomical changes induced by antipsychotic drugs are controversial. For instance, chronic haloperidol has been reported to both increase (Kerns *et al*, 1992) and decrease (Kelley *et al*, 1997) spine density in the rat striatum. To reexamine the question with advanced tools, the effects of chronic haloperidol administration on the dendritic morphology and physiology of identified iSPNs and dSPNs were studied using a combination of optogenetic, two-photon laser scanning microscopy and electrophysiological approaches in *ex vivo* brain slices from mice. These studies show that haloperidol treatment induces a slow remodeling of the corticostriatal indirect pathway implicated in the positive symptoms of schizophrenia.

*Correspondence: Dr D James Surmeier, Department of Physiology, Feinberg School of Medicine, Northwestern University, 303 E Superior, Chicago, IL 60611, USA, Tel: +1 312 503 4904, Fax: +1 312 503 5101, E-mail: j-surmeier@northwestern.edu
Received 23 September 2015; revised 8 August 2016; accepted 10 August 2016; accepted article preview online 31 August 2016

MATERIALS AND METHODS

Haloperidol Treatment

Male and female hemizygous bacterial artificial chromosome (BAC) transgenic mice (p28-p38) expressing eGFP under either *Drd1a* or *Drd2* control (Chan *et al*, 2012) were treated with intraperitoneally (IP) injected haloperidol-HCl (1 mg/kg) (Tocris Bristol, UK), perphenazine (4 mg/kg)

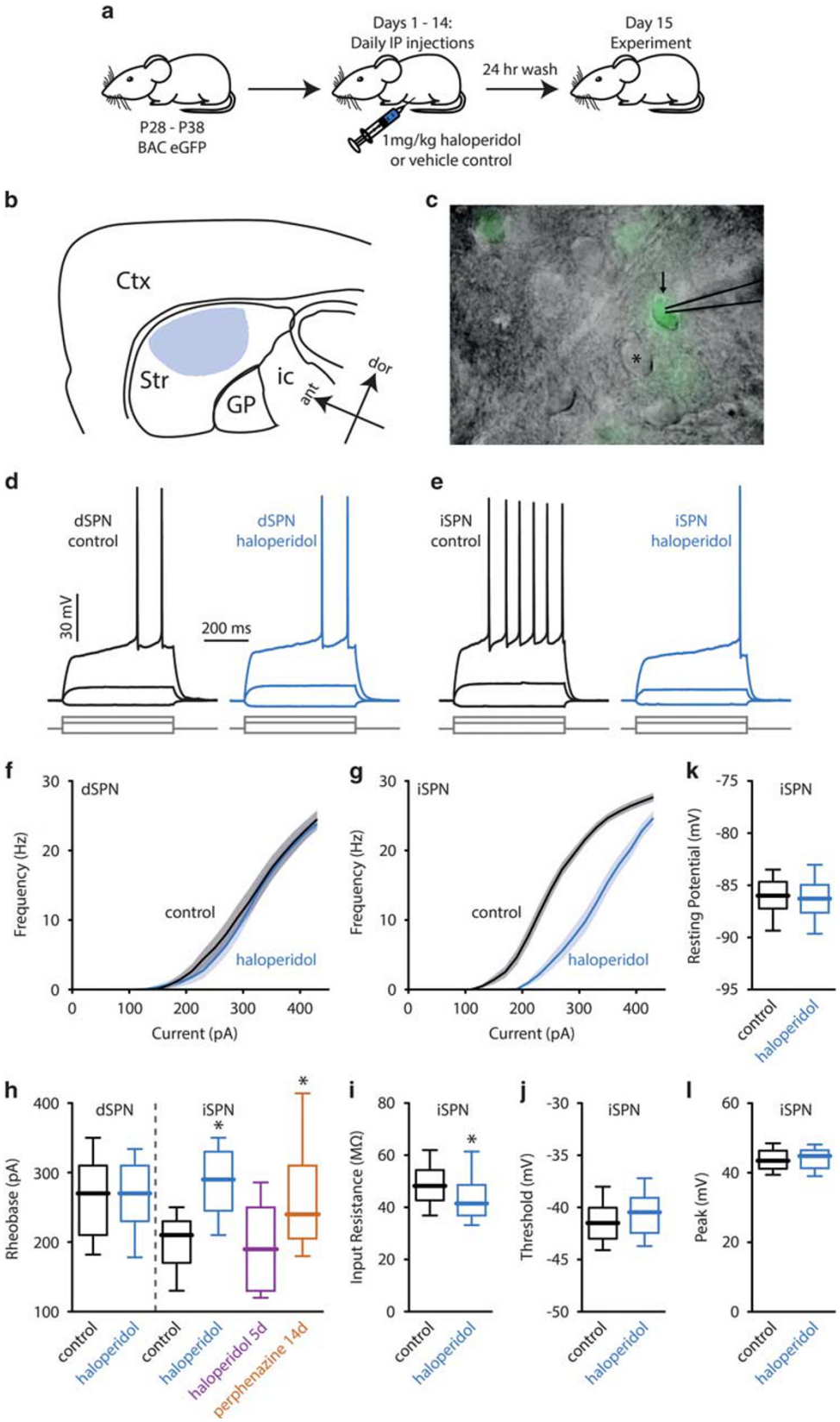

(Sigma-Aldrich, St Louis, MO), or 0.9% saline control for 14 days, except where otherwise noted (Figure 1a). We began injecting at postnatal week 5 to ensure adequate striatal development (Tepper *et al*, 1998). Injections were halted 24 h before experiments to ensure complete drug washout (Kirschbaum *et al*, 2008). In a subset of experiments, animals were injected with a single dose of haloperidol or 5 days of haloperidol before a 24 h washout before experimentation. A final subset of experiments used primed mini-osmotic pumps (Alzet, Cupertino, CA) to continuously deliver 0.25 mg/kg per day of haloperidol-HCl or vehicle control for 14 days, as previously described (Ilijic *et al*, 2011). Pumps were removed 24 h before experimentation. For circuit mapping experiments, *Drd2* eGFP mice were crossed with a transgenic line that expresses channelrhodopsin-2 in the cortex (Thy1-ChR2) (Fieblinger *et al*, 2014). All mice were housed on a 12 h light/dark schedule with food and water available *ad libitum*. All protocols described here were reviewed and approved by the Northwestern Institutional Animal Care and Use Committee and all efforts were made to minimize suffering.

Brain Slice Preparation

Following 24 h of washout (Figure 1a), mice were deeply anesthetized with a mixture of ketamine (50 mg/kg) and xylazine (4.5 mg/kg), and acute *ex vivo* brain slices were prepared as previously described (Chan *et al*, 2012) with the following modification: 240 μm parasagittal slices were taken by blocking the brain midsagittally and gluing medial side down on a ~15° agar block to preserve corticostriatal projections for electrical stimulation.

Whole-Cell Patch-Clamp Recording

Slices were transferred to a submersion-style recording chamber on a BX51 upright, fixed-stage microscope (Olympus, Center Valley, PA) and continuously superfused with aCSF containing the following (in mM): 125 NaCl, 2.5 KCl, 1.25 NaH_2PO_4, 25 $NaHCO_3$, 1 $MgCl_2$, 2 $CaCl_2$, and 13.9 D(+)-Glucose. Slices were visualized under differential interference contrast (DIC) and somatic eGFP expression was checked using epifluorescence microscopy to verify cell identity (Figure 1c). Thick-walled (1.5 mm outer diameter) borosilicate pipettes (Sutter Instrument Company, Novato, CA) were pulled on a Flaming/Brown micropipette puller (Sutter) and were 3–4 MΩ when filled with recording solution. Electrophysiological recordings were obtained with a MultiClamp 700 A amplifier interfaced with a PC running pClamp 10 (Molecular Devices, Sunnyvale, CA). Data were acquired at 50 kHz and filtered at 10 kHz except for Sr^{2+} miniature excitatory postsynaptic potentials (mEPSCs) that were filtered at 1 kHz, using an 8-pole Bessel filter and digitized using a DigiData 1322A A/D converter (Molecular Devices). The internal solution for current clamp recordings contained (in mM): 135 $KMeSO_4$, 5 KCl, 5 HEPES, 5 EGTA, 0.5 $CaCl_2$, 10 Na_2-phosphocreatine, 2 Mg-ATP, 0.5 Na-GTP, pH adjusted to 7.25–7.30 with NaOH, 300 mOsm. The amplifier bridge circuit was adjusted to account for serial resistance and was continuously monitored. For voltage clamp recordings the pipettes were filled with a Cs^+-based internal solution containing (in mM): 130 $CsMeSO_3$, 5 HEPES, 0.25 EGTA, 10 Na_2-phosphocreatine, 2 Mg-ATP, 0.5 Na-GTP, 5 TEA-Cl (tetraethylammonium-Cl), 1 QX-314-Cl, pH adjusted to 7.25–7.30 with CsOH, 290 mOsm. A 5 mV test pulse was continually monitored during voltage clamp recordings and cells with an access resistance of over 20 MΩ or whose resistance changed >20% were discarded. For experiments that employed cortical stimulation, a 200 μs pulse was delivered via a platinum/iridium parallel bipolar electrode (FHC, Bowdoin, ME) placed between layers V and VI of the cortex.

To determine the AP threshold, phase plots of the first derivative of somatic membrane potential (dV/dt) were constructed and the inflection point of the membrane potential (where the slope reached 10 mV/ms) was used as the threshold (Naundorf *et al*, 2006). Voltage–current plots were constructed from the equilibrium potentials reached for different somatic current injections (−150 to 90 pA, 20 pA increments). Sr^{2+} mEPSCs were recorded as previously described (Ding *et al*, 2008).

Subcellular Channelrhodopsin-Assisted Circuit Mapping (sCRACM)

Slices were taken from haloperidol- or saline-treated Thy1-ChR2-D2 mice and sCRACM was performed as previously described (Fieblinger *et al*, 2014) using standard aCSF supplemented with: 1.0 μM TTX, 100 μM 4-AP, 10 μM SR-95531 hydrobromide (gabazine), and 1.0 μM CGP 35348; 50 μM Alexa Fluor 568 hydrazide sodium salt was added to the Cs^+-based internal to allow visualization of spines.

Figure 1 Haloperidol decreased intrinsic excitability in iSPNs. (a) Example of haloperidol dosing schedule. (b) Schematic of a parasagittal (~15°) slice depicting the cortex (Ctx), striatum (Str), globus pallidus (GP), and internal capsule (ic); the region in blue indicates the area of interest where cells were assayed. Arrows signify anterior (ant) and dorsal (dor) axis orientation. (c) 40 × DIC image from a BAC D_2 eGFP animal with epifluorescence overlay (green) that shows a patch pipette (black lines) in contact with an iSPN (arrow) that is adjacent to a dSPN (asterisk). (d, e) Representative current-clamp recordings showing dSPNs and iSPNs treated with vehicle (black) or haloperidol (blue) for 14 days. The current injection protocol (diagram below) consisted of three 500 ms steps (−50, 90, and 290 pA). (f, g) dSPN intrinsic excitability was unchanged (control $n=25$, haloperidol $n=23$) and iSPN intrinsic excitability reduced (rightward shift in the current-response curve) by chronic haloperidol treatment (control $n=37$, haloperidol $n=34$). Shaded regions indicate SEM. (h) Following 14 days of haloperidol treatment, rheobase current did not change in dSPNs (control: 270 pA, $n=25$; haloperidol: 270 pA, $n=23$; Mann–Whitney test, $p=0.89$). In iSPNs, 5 days of haloperidol did not change rheobase, but 14-day (14d) treatment with either haloperidol or perphenazine increased rheobase (control: 210 pA, $n=37$; 5d haloperidol: 190 pA, $n=16$, $p=0.99$; 14d haloperidol: 290 pA, $n=34$, $p<0.0001$; 14d perphenazine: 240 pA, $n=20$, $p=0.01$; Kruskal–Wallis test with Dunn's correction). (i) Input resistance decreased in iSPNs (control: 48.22 MΩ, $n=37$; haloperidol: 41.53 MΩ, $n=34$; Mann–Whitney test, $p=0.02$). (j, k, l) Action potential (AP) threshold, resting membrane potential (RMP), and AP peak voltage were all unchanged in iSPNs following haloperidol (control AP threshold: −41.49 mV, $n=37$; haloperidol AP threshold: −40.46 mV, $n=34$; Mann–Whitney test, $p=0.17$; control RMP: −85.99 mV, $n=37$; haloperidol RMP: −86.27 mV, $n=34$; Mann–Whitney test, $p=0.48$; control AP peak: 43.49 mV, $n=37$; haloperidol AP peak: 44.82 mV, $n=34$; Mann–Whitney test, $p=0.63$). Asterisks indicate $p<0.05$.

Dendritic Reconstruction

For anatomical reconstructions, 0.2% biocytin was included in the recording solution and allowed to dialyze into the cell for at least 30 min during whole-cell patch-clamp. Slices were recovered and fixed in 4% paraformaldehyde for 12 h. Following 4 washes with phosphate-buffered saline (PBS), fixed slices were reacted with 2 μg/ml streptavidin-AlexaFluor 594 (Thermo Fisher Scientific, Waltham, MA) in PBS with 1% normal goat serum, 2% Triton-X for 12–18 h on a reciprocal shaker. Slices were washed 4 times with PBS and mounted on slides using ProLong Gold (Thermo Fisher Scientific). Slides were visualized on a 2PLSM setup using a 60X/1.2NA water immersion objective (Olympus). For whole-cell reconstructions, 0.5 μm serial optical sections (*Z*-stacks) were obtained with 0.386 μm^2 pixel resolution. Four *Z*-stacks per cell were stitched together using volume integration and alignment software (VIAS, Mt Sinai Computational Neurobiology and Imaging Center), and subsequently reconstructed and analyzed using Neurolucida (MicroBrightField, Williston, VT). For spine reconstructions, 0.15 μm *Z*-stacks with 0.132 μm^2 pixels were obtained from 2 proximal and 2 distal sections per cell. *Z*-stacks were deconvolved using AutoQuant (MediaCybernetics, Rockville, MD) and spines were counted in three dimensions semi-automatically using NeuronStudio (CNIC, Mount Sinai School of Medicine, New York, NY).

Gene Expression Profiling

Quantitative polymerase chain reaction (qPCR) was used as previously described (Chan *et al*, 2012; Plotkin *et al*, 2013, 2014) to determine the changes in transcript expression following haloperidol administration. In brief, the striatum from haloperidol- or control-treated animals was micro-dissected and iSPNs were separated out via fluorescence-assisted cell sorting (FACS) based on their eGFP expression. Total mRNA was isolated with the RNeasy Micro Kit (Qiagen, Valencia, CA) before synthesizing cDNA using qScript cDNA Supermix (Quanta Biosciences, Gaithersburg, MD). Real-time PCR was performed using Fast SYBR Mastermix (Applied Biosystems, Waltham, MA) on a StepOnePlus thermocycler (Applied Biosystems). The thermal cycling protocol began with a denaturing step at 95 °C for 20 s and then completed 40 cycles of 95 °C for 3 s and 60 °C for 30 s. The PCR cycle threshold (C_T) values were measured during the exponential phase of the PCR reaction and a comparative quantification method ($\Delta\Delta C_T$) was used to identify differences in gene expression level. An ensemble reference was calculated from the stability-based weighted C_Ts of a panel of reference genes (*Gapdh*, *Atp5b*, *Cyc1*, *Eif4az*, *Gusb*, *Hmbs*, *Actb*, *Uchl1*). Experiments for each gene of interest were run in triplicate to generate medians for comparison.

Data Analysis and Statistics

Data were analyzed using Clampfit 10 (Molecular Devices), Matlab (Mathworks, Natick, MA), and MiniAnalysis (Synaptosoft, Decatur, GA). Statistics were performed in Prism 6 (GraphPad, La Jolla, CA). Data are plotted as mean ± SEM and summary statistics are presented in box-and-whisker plots showing median, quartiles, and 10–90% range. Statistical analysis was performed using the nonparametric Mann–Whitney *U* and Kruskal–Wallis (with Dunn's multiple comparison *post hoc*) tests of significance. Data are considered significant when $p < 0.05$.

RESULTS

Haloperidol Diminished Intrinsic Excitability of iSPNs, But Not dSPNs

To investigate the effect of long-term antipsychotic administration on the striatum, BAC transgenic animals were used to allow the unambiguous identification of dSPNs and iSPNs in the slice via somatic eGFP expression using epifluorescence microscopy (Gertler *et al*, 2008). BAC mice were injected with the typical antipsychotic haloperidol or saline for 2 weeks and then whole-cell patch-clamp recordings were performed in *ex vivo* striatal slices. Intrinsic excitability was assessed by graded current injection in current-clamp mode. Haloperidol treatment had no effect on dSPN intrinsic excitability (Figures 1d, f and h). However, haloperidol treatment decreased the excitability of iSPNs (Figures 1e and g), a change reflected in a greater rheobase current (the amount of current needed to produce at least one action potential, assessed in 20 pA increments) (Figure 1h).

To ensure that the effect seen in iSPNs was a long-term adaptation, rather than an acute effect of haloperidol, previously untreated mice were injected with a single dose of haloperidol and recorded from 24 h later. In this case, there were no differences found in the intrinsic excitability of iSPNs (Supplementary Figure S1). To further characterize the time course of the effect, rheobase was measured in iSPNs from mice treated for 5 days (rather than 14); at this time point, rheobase was unchanged (Figure 1h). To determine whether the effect was specific to haloperidol, the typical antipsychotic perphenazine was administered. Perphenazine is a medium-potency phenothiazine antipsychotic that antagonizes D_2 receptors. Fourteen days of perphenazine administration had a similar effect on rheobase as 14 days of haloperidol (Figure 1h).

Work in rats has suggested that administration of antipsychotics with osmotic mini-pumps rather than IP injections may more accurately mimic human dosing, as assessed by *in vivo* D_2R occupancy (Kapur *et al*, 2003). For this reason, the 2-week administration was repeated using osmotic mini-pumps to deliver haloperidol (0.25 mg/kg per day). The results using this delivery method reproduced the drop in intrinsic excitability found using IP injections (Supplementary Figure S2).

To better understand the mechanism underlying the change in excitability seen in iSPNs, input resistance, action potential (AP) threshold, resting membrane potential (RMP), and peak AP voltage were measured. The input resistance was calculated from the slope of the best-fit line of the steady-state voltages obtained following a series of hyperpolarizing somatic current injections (−150 to −70 pA, 20 pA intervals). Using this method, the input resistance for iSPNs in haloperidol-treated animals was significantly less than that of controls, but the AP threshold, RMP, and AP peak were all unchanged (Figures 1i–l).

Kir2 K^+ Channel Currents Were Increased by Haloperidol Treatment

The Kir2 family of inward rectifying K^+ channels are major determinants of the resting conductance and basal excitability of SPNs (Mermelstein *et al*, 1998; Nisenbaum and Wilson, 1995; Uchimura *et al*, 1989). To determine whether Kir2 K^+ channel expression was altered by haloperidol treatment, iSPNs from treated and control mice were isolated using FACS and then qPCR was performed (Chan *et al*, 2012; Plotkin *et al*, 2013, 2014). The abundance of Kir2.3 mRNA was increased by haloperidol treatment, but Kir2.1, 2.2, and 2.4 mRNAs were unchanged (Figure 2a).

Voltage-clamp recordings of iSPNs from haloperidol- or vehicle-treated animals were performed to see whether Kir2.3 mRNA upregulation resulted in increased protein and current. Voltage–current plots from control- and haloperidol treated animals revealed a divergence around the K^+ equilibrium potential, suggesting that Kir channel currents were increased by haloperidol treatment (Figure 2b). To provide an additional test of this hypothesis, somatic voltage ramps (−150 to −30 mV, 200 ms) were performed and difference currents were computed; these difference currents had a reversal near the K^+ equilibrium potential and demonstrated inward rectification, both typical features of Kir2 channels (Figure 2c). Finally, iSPNs were voltage-clamped at −60 mV (inactivating Kv1 and Kv4 channels but leaving Kir2 channels open) and then stepped to −130 mV; control- and haloperidol-treated iSPNs revealed a difference in the maximum current (Figures 2d and e). These results are all consistent with the hypothesis that the upregulation of Kir2.3 mRNA found in haloperidol-treated animals resulted in increased Kir2 channel currents and reduced intrinsic excitability of iSPNs.

It is possible that other mechanisms also contribute to the drop in excitability seen following chronic haloperidol treatment. Lesioning dopaminergic neurons caused a shrinkage of SPN dendrites (Fieblinger *et al*, 2014) and D_2R overexpression resulted in an expanded dendritic arbor (Cazorla *et al*, 2012). To determine whether there were dendritic changes following haloperidol treatment, iSPNs from treated and control animals were reconstructed and Sholl analysis was performed (Supplementary Figures S3A–C). The total dendritic length of iSPNs was unchanged by haloperidol treatment (Supplementary Figure S3D). Proximal dendritic morphology has a greater impact on somatically assessed excitability than distal morphology, and hence remodeling without a change in the total length could still conceivably affect excitability. However, haloperidol treatment did not change the number of primary dendrites, nodes, or terminal dendritic branches (Supplementary Figures S3E–G). Thus, dendritic remodeling does not appear to contribute to the drop in excitability seen in iSPNs following chronic haloperidol exposure.

Haloperidol Decreased Spine Density

Loss of dopaminergic signaling has been shown to cause a selective reduction in iSPN spine density (Day *et al*, 2006; Fieblinger *et al*, 2014). Studies of chronic haloperidol administration show less consensus, with some reporting decreased spine density in SPNs (Kelley *et al*, 1997; Roberts

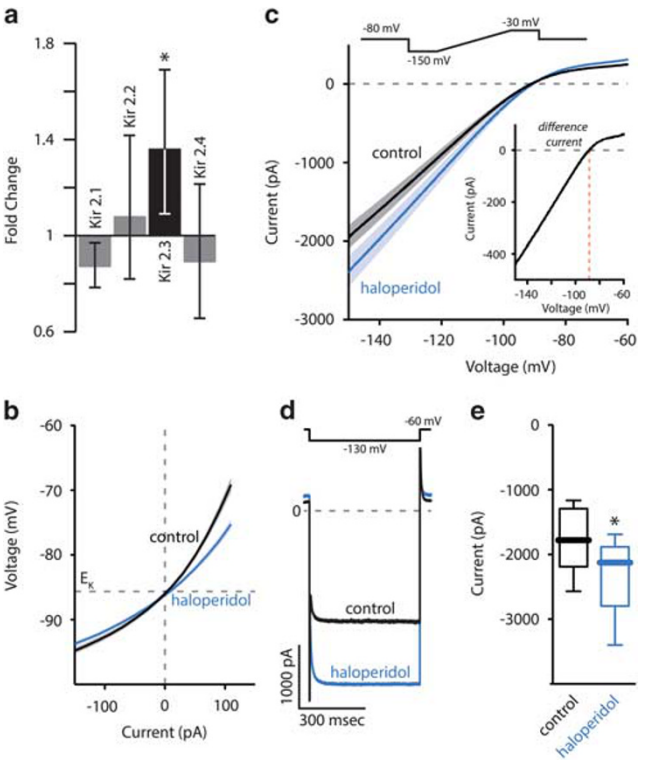

Figure 2 Haloperidol treatment caused Kir2.3 upregulation and increased Kir2-mediated currents. (a) qPCR was performed on iSPNs isolated via their eGFP expression using fluorescence-activated cell sorting. Data are presented as fold change (FC) calculated from $\Delta\Delta C_T$ values. Only Kir2.3 was significantly increased in the haloperidol group (Kir2.1 FC: 0.87, $p = 0.33$; Kir2.2 FC: 1.08, $p = 0.36$; Kir2.3 FC: 1.36, $p = 0.001$; Kir2.4 FC: 0.89, $p = 0.80$; control $n = 13$, haloperidol $n = 13$; Mann–Whitney test). Dark shading indicates significance. (b) Voltage–current plot determined from current steps in voltage-clamp mode. iSPNs were recorded in control (black) and haloperidol-treated (blue) animals. Shading indicates SEM. (c) Mean current response to a 200 ms voltage ramp (from −150 to −30 mV, inset, top). The difference current is also shown (inset, right). (d, e) Haloperidol increased the peak inward current measured by stepping cells from a holding potential of −60 to −130 mV (control: −1779 pA, $n = 9$; haloperidol −2126 pA, $n = 9$; Mann–Whitney test, $p = 0.03$). Asterisk indicates $p < 0.05$.

et al, 1995), and others increased spine density (Kerns *et al*, 1992). However, none of the haloperidol studies distinguished between iSPNs and dSPNs that would be expected to have a major impact on the outcome. Using BAC transgenic mice, identified iSPNs were filled with biocytin using a patch electrode, fixed, optically sectioned using 2PLSM, and then reconstructed in 3D using standard approaches (Dumitriu *et al*, 2011; Gertler *et al*, 2008). Both proximal (centered at 50 μm from the soma) and distal (centered at 110 μm) segments of dendrite were examined and estimates of spine density were generated (Figures 3a and b). Haloperidol administration decreased the median spine density of both proximal and distal iSPN dendrites; this drop was evident at 5 days of treatment and persisted through 14 days of treatment (Figure 3c). Although median spine densities were similar at proximal and distal locations, the variability of the measurements was considerably less in distal dendrites, suggesting the effect was more robust. Perphenazine treatment (14 days) also was effective in decreasing spine density of iSPNs (Figure 3c).

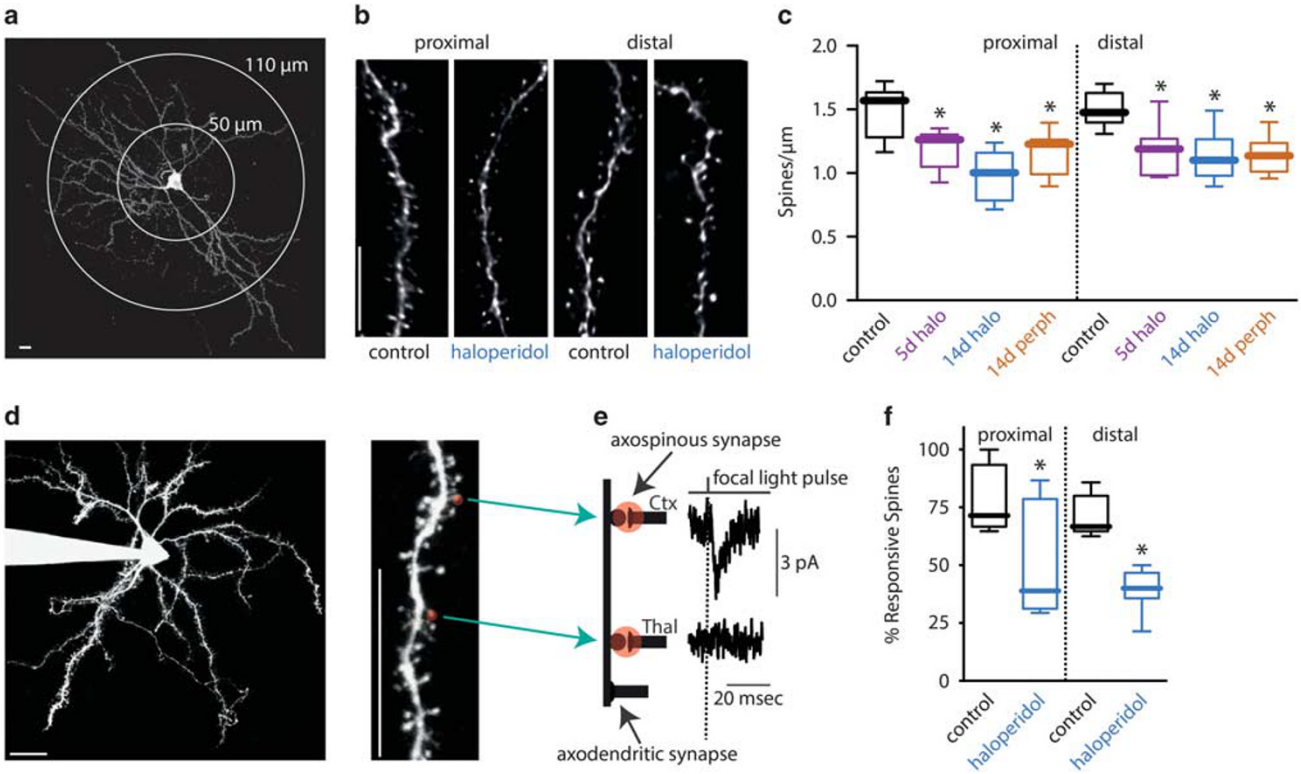

Figure 3 Haloperidol induced the loss of cortically responsive spines. (a) A maximum intensity projection (MIP) of a biocytin-stained iSPN from a vehicle-injected D_2 eGFP animal. Concentric circles indicate the proximal (50 µm from the soma) and distal distances (>90 µm from the soma) for spine counting and subcellular channelrhodopsin-assisted circuit mapping (sCRACM). (b) Representative deconvolved MIPs of dendritic segments used for spine counting. (c) Spine density decreased in both proximal and distal regions with 5 days (5d) of haloperidol (proximal: control = 1.56 spines/µm, $n = 8$; 5d haloperidol = 1.26 spines/µm, $n = 15$, $p = 0.05$; distal: control = 1.48 spines/µm, $n = 8$; 5d haloperidol = 1.19 spines/µm, $n = 15$, $p = 0.004$, Kruskal–Wallis test with Dunn's correction), with 14 days (14d) of haloperidol (proximal: control = 1.56 spines/µm, 14d haloperidol = 1.00 spines/µm, $p = 0.001$; distal: control = 1.48 spines/µm, 14d haloperidol = 1.10 spines/µm, $p = 0.008$; control $n = 8$, 14d haloperidol $n = 6$, Kruskal–Wallis test with Dunn's correction), and with 14 days (14d) of perphenazine (proximal: control = 1.56 spines/µm, 14d perphenazine = 1.23 spines/µm, $p = 0.011$; distal: control = 1.48 spines/µm, 14d perphenazine = 1.14 spines/µm, $p < 0.001$; control $n = 8$, 14d perphenazine $n = 16$, Kruskal–Wallis test with Dunn's correction). (d) Sample 2PLSM MIP of an iSPN (left) that was patch-clamped and dialyzed with Alexa Fluor 568 and a region of dendrite (right) targeted for sCRACM. Red circles indicate regions sampled for focal blue laser stimulation of ChR2. (e) A cartoon representation (left) of the region of dendrite shown in (d). Somatic voltage records (right) in response to focal laser stimulation; when laser stimulation produced a response the spines were classified as cortically responsive. (f) Haloperidol treatment reduced the percent of cortical-responsive spines in both regions examined (proximal: control = 71.43%, haloperidol = 38.89%, $p = 0.038$; distal: control = 66.67%, haloperidol = 40.00, $p = 0.0006$; control $n = 7$, haloperidol $n = 7$, Mann–Whitney test). Scale bars, 10 µm; asterisks indicate $p < 0.05$.

SPNs receive excitatory glutamatergic innervation from both the cerebral cortex and thalamus. However, the majority of axospinous synapses are cortical in origin (Smith *et al*, 2004). To determine whether cortical axospinous synapses were being lost following haloperidol treatment, the sCRACM approach was used (Fieblinger *et al*, 2014; Petreanu *et al*, 2009). This method uses focal illumination of spine heads imaged using 2PLSM in *ex vivo* brain slices. When illuminated, presynaptic terminals expressing channelrhodopsin (ChR2) depolarize and release neurotransmitter, generating a postsynaptic current detected by a somatic patch electrode. By expressing ChR2 in presynaptic terminals of a given type, the terminals can be mapped. To map corticostriatal synapses onto iSPNs, Thy1-ChR2 mice that express channelrhodopsin in corticostriatal but not thalamostriatal neurons were crossed with D_2 eGFP mice (Plotkin *et al*, 2014). These mice were treated with haloperidol or vehicle control. After treatment, brain slices were prepared and iSPNs were patched and filled with an Alexa dye to allow the visualization of dendrites. Spines were then interrogated with a blue laser to determine whether a cortical terminal was present (Figures 3d and e). In control iSPNs, roughly 70% of the spines on proximal and distal dendrites had detectable cortical synapses; this is in good agreement with previous results using this approach and anatomical estimates of corticostriatal synapse density (Fieblinger *et al*, 2014; Plotkin *et al*, 2014; Smith *et al*, 2009; Villalba and Smith, 2011). After haloperidol treatment, this percentage dropped to ~40% in both proximal and distal dendrites (Figure 3f). These results suggest that there was a selective pruning of cortical synapses by haloperidol treatment.

Haloperidol Increased the Strength of Remaining Axospinous Synapses

Activation of D_2Rs is necessary for endocannabinoid (eCB)-mediated long-term synaptic depression (LTD) in the striatum (Gerfen and Surmeier, 2011; Kreitzer and Malenka, 2007). In this form of plasticity, retrograde signaling of eCBs activates presynaptic cannabinoid 1 receptors that decrease release probability. Chronic blockade

of D_2Rs by haloperidol might blunt normal eCB-LTD induction, leading to de-depression of corticostriatal synapses. To assess this possibility, the paired-pulse ratio (PPR), which can indicate changes in release probability (Zucker and Regehr, 2002), was measured in iSPNs in response to electrical stimulation of corticostriatal fibers (Figure 4a). As would be expected from the loss of eCB-LTD, the PPR in iSPNs was significantly lower in haloperidol-treated animals than in vehicle controls (Figure 4b), indicating an increased probability of release.

To determine whether synaptic strength was affected by haloperidol treatment, asynchronous corticostriatal mEPSCs were evoked by electrical stimulation of corticostriatal axons in aCSF containing Sr^{2+} in place of Ca^{2+} (Ding *et al*, 2008) (Figures 4c and d); Sr^{2+} replacement increases asynchronous quantal release, allowing mEPSCs of known presynaptic origin to be determined (Choi and Lovinger, 1997). Although the frequency of asynchronous mEPSCs is not readily related to release probability, the amplitude of mEPSCs provides a direct measure of synaptic strength. Because postsynaptic glutamate receptors at this synapse are not saturated normally (Higley *et al*, 2009), an elevation in presynaptic release probability could result in an increase in mEPSC amplitude. Indeed, the average corticostriatal mEPSC amplitude in iSPNs was increased by haloperidol treatment, suggesting a loss of presynaptic eCB-LTD (Figures 4e and f; Supplementary Figure S4). In addition, analysis of corticostriatal synaptic strength obtained via optogenetic stimulation in Thy1-ChR2 mice revealed an increase in the median amplitude of response following haloperidol treatment (control: 4.3 pA, $n = 134$ spines; haloperidol: 5.3 pA, $n = 95$ spines; Mann–Whitney *U*-test; $p = 0.004$) that was roughly equivalent (~25%) to that seen with Sr^{2+} mEPSCs.

Finally, the ratio of *N*-methyl-D-aspartate receptor (NMDAR) currents to α-amino-3-hydroxy-5-methyl-4-isoxazolepropionic acid receptor (AMPAR) currents at corticostriatal synapses was measured using an established technique (Myme *et al*, 2003) (Supplementary Figure S5A). This ratio is often used as a means of determining whether postsynaptic long-term depression or potentiation, which changes the relative abundance of synaptic AMPARs, has occurred (Yang and Calakos, 2013). The time course of AMPAR currents was first determined at −80 mV, a potential at which Mg^{2+} blocks NMDAR currents. Then the cortex was stimulated while holding the cell at +40 mV to reveal NMDAR currents in addition to AMPAR currents. The AMPAR component was taken at the time of peak AMPAR current assessed at −80 mV, whereas the NMDAR component was taken 40 ms later, after the AMPAR current had completely decayed (Supplementary Figure S5A). Using this technique, haloperidol treatment did not change the synaptic NMDA/AMPA current ratio (Supplementary Figure S5B), suggesting a presynaptic mechanism of action.

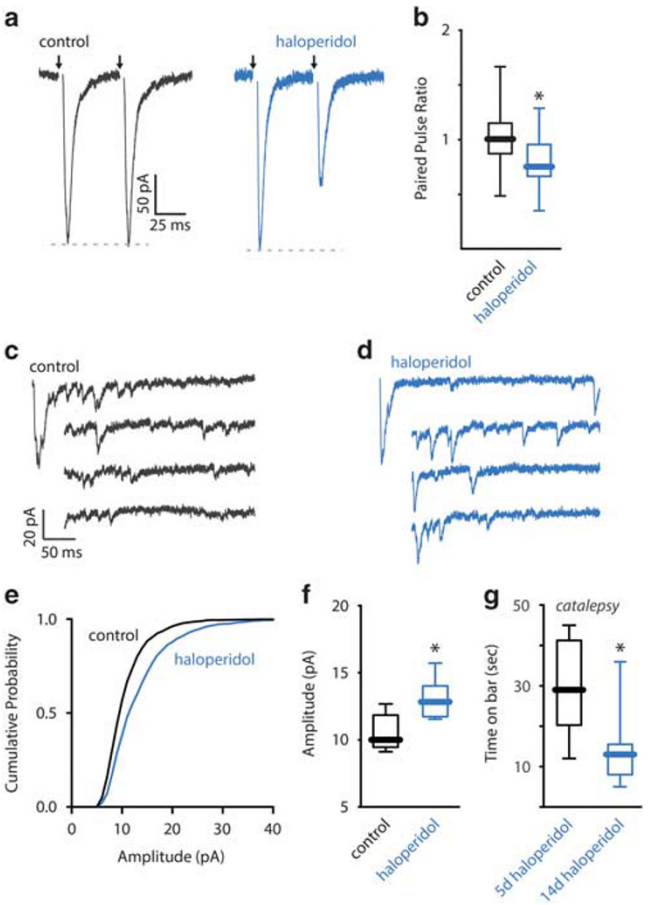

Figure 4 Haloperidol strengthened the remaining corticostriatal synapses. (a) Representative EPSCs evoked by paired-pulse (20 Hz) electrical stimulation of the cortex. Arrows denote cortical stimuli. (b) The PPR in controls was mildly facilitating but was depressing in haloperidol animals, indicating an increased probability of release (control: 1.00, $n = 25$; haloperidol: 0.75, $n = 19$; Mann–Whitney test, $p = 0.007$). Representative traces showing asynchronous release evoked by cortical stimulation measured in iSPNs of control (c) and haloperidol-treated (d) animals. (e) Cumulative probability distribution of mEPSC amplitude. (f) Haloperidol increased mEPSC amplitude as compared with control (control: 10.01 pA, $n = 8$; haloperidol: 12.83 pA, $n = 7$; Mann–Whitney test, $p = 0.004$). (g) Mice developed tolerance to catalepsy following 14 days of haloperidol administration (time on bar: 5d haloperidol: 29 s, $p = 8$; 14d haloperidol: 13 s, $n = 9$; Mann–Whitney test, $p = 0.007$). Asterisks indicate $p < 0.05$.

Haloperidol Tolerance Paralleled Adaptations in iSPNs

Catalepsy is a basal ganglia-mediated behavior that can be triggered by antipsychotic administration (Bateup *et al*, 2010). Tolerance to the cataleptic effects of haloperidol develops with repeated treatment (Ezrin-Waters and Seeman, 1977). To determine whether the development of tolerance paralleled the adaptations in iSPNs, mice were treated for 5 or 14 days with haloperidol and their tolerance to catalepsy measured using a standard test (Peterson *et al*, 2012). The cataleptic tolerance to haloperidol was progressive, increasing significantly from 5 to 14 days of treatment (Figure 4g), paralleling the changes in intrinsic excitability of iSPNs.

DISCUSSION

This study shows that chronic (2 weeks) treatment of mice with haloperidol induces a concerted set of adaptations specifically in striatal iSPNs. Although haloperidol is a nonselective, albeit preferential, D_2 receptor antagonist (Bymaster *et al*, 1996), both the downregulation of intrinsic excitability and of excitatory synaptic connectivity with

cortical pyramidal neurons appear to reflect a form of homeostatic plasticity triggered by the loss of tonic, inhibitory D_2R-mediated modulation of iSPNs. These homeostatic adaptations should serve to normalize the average spiking rate of iSPNs following neuroleptic treatment, diminishing the propensity of this network to indiscriminately suppress goal-directed movement and habits. However, in parallel, neuroleptic treatment led to the strengthening of a subset of corticostriatal synapses, increasing their ability to drive iSPN activity. Thus, chronic neuroleptic treatment leads to a reorganization of the corticostriatal circuitry controlling active suppression of thoughts and movements. Whereas the changes in synaptic density occurred rapidly, alterations in intrinsic excitability were slower. Although our behavioral data indicate that the changes in intrinsic excitability parallels tolerance to catalepsy, the time course of these adaptations also mirrors the delay between neuroleptic administration and therapeutic benefit; further study in a rodent model of schizophrenia would be of value to determine whether the reported iSPN adaptations are also associated with symptoms of schizophrenia, particularly positive symptoms.

Homeostatic Adaptations to Chronic Haloperidol

D_2R signaling has both rapid and slow neuromodulatory effects on iSPNs. The rapid neuromodulatory effects of D2R signaling are mediated by $G_{i/o}$ proteins coupled to adenylyl cyclase and phospholipase C, leading to altered gating of Na^+, Ca^{2+}, and K^+ channels (Gerfen and Surmeier, 2011). The same signaling pathways mediate slow, lasting downregulation of excitatory synaptic connections (Gerfen and Surmeier, 2011; Kreitzer and Malenka, 2007). Thus, both slow and fast effects of D_2R signaling tend to decrease the activity of iSPNs. How then does chronic haloperidol treatment, which should decrease inhibitory D_2R signaling, lead to a drop in iSPN excitability? By attenuating tonic inhibitory D_2R signaling in iSPNs, haloperidol should increase their spiking rate (West and Grace, 2002; Zhang and Linden, 2003). With high doses of haloperidol, this disinhibition of iSPNs broadly suppresses movement, inducing catalepsy. However, sustained deviations of spike rate away from a neuron's predetermined set-point induces homeostatic compensation or plasticity (Marder and Goaillard, 2006; Turrigiano, 2008). Two forms of homeostatic plasticity have been described: intrinsic and synaptic. Intrinsic homeostatic plasticity leads to alterations in postsynaptic ion channel expression and function that control spike generation. Synaptic homeostatic plasticity or scaling leads to changes in the strength of excitatory glutamatergic synapses that drive neurons to spike.

In the case of iSPNs, sustained antagonism of inhibitory D_2R signaling should engage a negative form of homeostatic plasticity that lowers, and hence normalizes, spiking rate. Indeed this is what was found. In iSPNs from mice treated with haloperidol, the ability to generate spikes from intrasomatic current injection was decreased and change paralleled the development of tolerance to catalepsy. This drop in excitability was attributable in part to an upregulation in the expression and function of Kir2.3K^+ channels. Both mRNA for this key subunit of Kir2 channels and Kir2 channel currents were upregulated by haloperidol treatment. This observation is consistent with recent work showing that upregulation of D_2R expression increased SPN excitability by downregulating Kir2 channel function (Cazorla *et al*, 2012).

In addition to intrinsic homeostatic plasticity, iSPNs from haloperidol-treated mice also pruned excitatory, glutamatergic axospinous synapses on both proximal and distal dendrites that can be interpreted as a form of synaptic homeostatic plasticity. This pruning was similar to that seen following striatal dopamine depletion (Day *et al*, 2006; Fieblinger *et al*, 2014). The pruning induced by haloperidol treatment appeared to occur primarily at corticostriatal, axospinous synapses, like that seen following dopamine depletion. However, rather than all excitatory synapses simply being downregulated (scaling) to maintain relative synaptic strength and the information embedded in these weights (Turrigiano, 2008), a subset of axospinous synapses were eliminated and others strengthened, as judged by the increase in Sr^{2+} mEPSC amplitude following haloperidol treatment. The strengthening of these synapses is attributable to dedepression following the loss of D_2R-dependent, presynaptic LTD (Gerfen and Surmeier, 2011). Consistent with a presynaptic locus for this change, the NMDAR/AMPAR current ratio—a commonly used measure of postsynaptic plasticity—was unaltered at corticostriatal synapses following haloperidol treatment. Moreover, the PPR at this synapse decreased, suggesting an increase in glutamate release probability, as expected following a loss of presynaptic LTD. This inference is consistent with ultrastructural studies showing that chronic haloperidol treatment increases the number of perforated striatal synapses (Meshul and Casey, 1989; Meshul *et al*, 1996), providing a structural foundation for our physiological observations (Calverley and Jones, 1990; Higley *et al*, 2009).

It remains to be seen how SPN homeostatic plasticity is regulated, but one potential mechanism is through Cav1 (L-type) Ca^{2+} channels that are robustly expressed by SPNs. Several studies have implicated Cav1 channels in the regulation of homeostatic plasticity (Turrigiano, 2008). This possibility is of considerable interest, as genome-wide association studies have implicated Cav1 polymorphisms in psychiatric diseases, particularly schizophrenia (Cross-Disorder Group of the Psychiatric Genomics Consortium, 2013).

Do Cholinergic Interneurons Contribute to the Effects of Haloperidol?

D_2R expression is not limited to iSPNs in the striatum. It is possible that these other cell types shape the iSPN adaptations to chronic haloperidol. The most probable participant in the response to haloperidol are D_2R-expressing cholinergic interneurons (ChIs). D_2R signaling in these neurons suppresses their ongoing pacemaking activity and acetylcholine release (Aosaki *et al*, 1994; Ding *et al*, 2010; Maurice *et al*, 2004; Stoof and Kebabian, 1982). Acetylcholine has a variety of striatal effects, but the most relevant in this context is the elevation in iSPN intrinsic excitability mediated by suppression of Kv7 (KCNQ) and Kir2 K^+ channels (Galarraga *et al*, 1999; Shen *et al*, 2005, 2007). It is possible that neuroleptic-induced elevation in cholinergic signaling contributes to the observed adaptations in iSPNs (Shen *et al*, 2007). However, *in vivo* microdialysis in

rodents chronically treated with haloperidol have found no change in basal ACh tone (Osborne *et al*, 1994).

Implications for Schizophrenia

Typical neuroleptics are most effective in reducing the positive symptoms of schizophrenia. These symptoms are thought to arise from hyperactivity of D_2R signaling and hypoexcitability of the indirect pathway—a key part of the brain circuitry that suppresses contextually inappropriate ideation, habits, and goal-directed activity. In principle, neuroleptics should immediately alleviate these symptoms if this simple model is correct. However, they do not, suggesting that there is something else awry in the schizophrenic brain. What this model lacks is an appreciation for the homeostatic potential of iSPNs. Cazorla *et al* (2012) show that sustained upregulation in D2R signaling, as might be found in schizophrenia, induces homeostatic alterations in the Kir2-dependent integrative mechanisms of SPNs. Our results suggest that haloperidol, and other typical antipsychotics such as perphenazine, can reverse these Kir2-dependent adaptations, but this reversal takes days or weeks.

In addition, there are compelling reasons to think that synaptic dysfunction contributes to the schizophrenic phenotype (Faludi and Mirnics, 2011; Mirnics *et al*, 2006). In agreement with this view, long-term antipsychotic treatment remodels axospinous machinery controlling corticostriatal synaptic function (Critchlow *et al*, 2006; Faludi and Mirnics, 2011; Lidow *et al*, 2001). Our results add an important dimension to this literature, showing that haloperidol slowly remodels corticostriatal circuitry controlling iSPNs, eliminating many synapses but strengthening others.

What remains to be determined are the types of corticostriatal synapses pruned and the types strengthened by haloperidol treatment. These might arise from different cortical regions or circuits. Our current hypothesis is that the axospinous synapses capable of undergoing synaptic plasticity (LTP) are selectively preserved. This would mean that the pruned synapses are not as sensitive to the consequences of choice that is signaled to the striatum by the dopaminergic neurons of the substantia nigra. By preferentially eliminating these synapses, haloperidol might force the activity of iSPNs to be more effectively governed by cortical inputs shaped by external events.

FUNDING AND DISCLOSURE

The authors declare no conflict of interest.

ACKNOWLEDGMENTS

We thank Dr Tracy Gertler for her contribution to the early stages of this project, Alexandria Melendez for auxiliary experiments, and Sasha Ulrich for technical assistance. This work was supported by NIMH P50 MH090963, NS34696, NS084735, and the JPB Foundation.

REFERENCES

Agid O, Kapur S, Arenovich T, Zipursky RB (2003). Delayed-onset hypothesis of antipsychotic action: a hypothesis tested and rejected. *Arch Gen Psychiatry* **60**: 1228–1235.

Aosaki T, Graybiel AM, Kimura M (1994). Effect of the nigrostriatal dopamine system on acquired neural responses in the striatum of behaving monkeys. *Science* **265**: 412–415.

Bateup HS, Santini E, Shen W, Birnbaum S, Valjent E, Surmeier DJ *et al* (2010). Distinct subclasses of medium spiny neurons differentially regulate striatal motor behaviors. *Proc Natl Acad Sci USA* **107**: 14845–14850.

Bymaster FP, Calligaro DO, Falcone JF, Marsh RD, Moore NA, Tye NC *et al* (1996). Radioreceptor binding profile of the atypical antipsychotic olanzapine. *Neuropsychopharmacology* **14**: 87–96.

Calverley RK, Jones DG (1990). Contributions of dendritic spines and perforated synapses to synaptic plasticity. *Brain Res Brain Res Rev* **15**: 215–249.

Cazorla M, Shegda M, Ramesh B, Harrison NL, Kellendonk C (2012). Striatal D2 receptors regulate dendritic morphology of medium spiny neurons via Kir2 channels. *J Neurosci* **32**: 2398–2409.

Centonze D, Usiello A, Costa C, Picconi B, Erbs E, Bernardi G *et al* (2004). Chronic haloperidol promotes corticostriatal long-term potentiation by targeting dopamine D2L receptors. *J Neurosci* **24**: 8214–8222.

Chan CS, Peterson JD, Gertler TS, Glajch KE, Quintana RE, Cui Q *et al* (2012). Strain-specific regulation of striatal phenotype in Drd2-eGFP BAC transgenic mice. *J Neurosci* **32**: 9124–9132.

Choi S, Lovinger DM (1997). Decreased frequency but not amplitude of quantal synaptic responses associated with expression of corticostriatal long-term depression. *J Neurosci* **17**: 8613–8620.

Creese I, Burt DR, Snyder SH (1976). Dopamine receptor binding predicts clinical and pharmacological potencies of antischizophrenic drugs. *Science* **192**: 481–483.

Critchlow HM, Maycox PR, Skepper JN, Krylova O (2006). Clozapine and haloperidol differentially regulate dendritic spine formation and synaptogenesis in rat hippocampal neurons. *Mol Cell Neurosci* **32**: 356–365.

Cross-Disorder Group of the Psychiatric Genomics Consortium (2013). Identification of risk loci with shared effects on five major psychiatric disorders: a genome-wide analysis. *Lancet* **381**: 1371–1379.

Day M, Wang Z, Ding J, An X, Ingham CA, Shering AF *et al* (2006). Selective elimination of glutamatergic synapses on striatopallidal neurons in Parkinson disease models. *Nat Neurosci* **9**: 251–259.

Ding J, Peterson JD, Surmeier DJ (2008). Corticostriatal and thalamostriatal synapses have distinctive properties. *J Neurosci* **28**: 6483–6492.

Ding JB, Guzman JN, Peterson JD, Goldberg JA, Surmeier DJ (2010). Thalamic gating of corticostriatal signaling by cholinergic interneurons. *Neuron* **67**: 294–307.

Dumitriu D, Rodriguez A, Morrison JH (2011). High-throughput, detailed, cell-specific neuroanatomy of dendritic spines using microinjection and confocal microscopy. *Nat Protoc* **6**: 1391–1411.

Ezrin-Waters C, Seeman P (1977). Tolerance of haloperidol catalepsy. *Eur J Pharmacol* **41**: 321–327.

Faludi G, Mirnics K (2011). Synaptic changes in the brain of subjects with schizophrenia. *Int J Dev Neurosci* **29**: 305–309.

Fieblinger T, Graves SM, Sebel LE, Alcacer C, Plotkin JL, Gertler TS *et al* (2014). Cell type-specific plasticity of striatal projection neurons in parkinsonism and L-DOPA-induced dyskinesia. *Nat Commun* **5**: 5316.

Frank MJ (2011). Computational models of motivated action selection in corticostriatal circuits. *Curr Opin Neurobiol* **21**: 381–386.

Galarraga E, Hernández-López S, Reyes A, Miranda I, Bermudez-Rattoni F, Vilchis C *et al* (1999). Cholinergic modulation of neostriatal output: a functional antagonism between different types of muscarinic receptors. *J Neurosci* **19**: 3629–3638.

Gerfen CR, Surmeier DJ (2011). Modulation of striatal projection systems by dopamine. *Annu Rev Neurosci* **34**: 441–466.

Gertler TS, Chan CS, Surmeier DJ (2008). Dichotomous anatomical properties of adult striatal medium spiny neurons. *J Neurosci* **28**: 10814–10824.

Higley MJ, Soler-Llavina GJ, Sabatini BL (2009). Cholinergic modulation of multivesicular release regulates striatal synaptic potency and integration. *Nat Neurosci* **12**: 1121–1128.

Ilijic E, Guzman JN, Surmeier DJ (2011). The L-type channel antagonist isradipine is neuroprotective in a mouse model of Parkinson's disease. *Neurobiol Dis* **43**: 364–371.

Kapur S, VanderSpek SC, Brownlee BA, Nobrega JN (2003). Antipsychotic dosing in preclinical models is often unrepresentative of the clinical condition: a suggested solution based on in vivo occupancy. *J Pharmacol Exp Ther* **305**: 625–631.

Kelley JJ, Gao XM, Tamminga CA, Roberts RC (1997). The effect of chronic haloperidol treatment on dendritic spines in the rat striatum. *Exp Neurol* **146**: 471–478.

Kerns JM, Sierens DK, Kao LC, Klawans HL, Carvey PM (1992). Synaptic plasticity in the rat striatum following chronic haloperidol treatment. *Clin Neuropharmacol* **15**: 488–500.

Kirschbaum KM, Henken S, Hiemke C, Schmitt U (2008). Pharmacodynamic consequences of P-glycoprotein-dependent pharmacokinetics of risperidone and haloperidol in mice. *Behav Brain Res* **188**: 298–303.

Konradi C, Heckers S (2001). Antipsychotic drugs and neuroplasticity: insights into the treatment and neurobiology of schizophrenia. *Biol Psychiatry* **50**: 729–742.

Kreitzer AC, Malenka RC (2007). Endocannabinoid-mediated rescue of striatal LTD and motor deficits in Parkinson's disease models. *Nature* **445**: 643–647.

Laruelle M, Kegeles LS, Abi-Dargham A (2003). Glutamate, dopamine, and schizophrenia: from pathophysiology to treatment. *Ann NY Acad Sci* **1003**: 138–158.

Leucht S, Busch R, Hamann J, Kissling W, Kane JM (2005). Early-onset hypothesis of antipsychotic drug action: a hypothesis tested, confirmed and extended. *Biol Psychiatry* **57**: 1543–1549.

Lidow MS, Song ZM, Castner SA, Allen PB, Greengard P, Goldman-Rakic PS (2001). Antipsychotic treatment induces alterations in dendrite- and spine-associated proteins in dopamine-rich areas of the primate cerebral cortex. *Biol Psychiatry* **49**: 1–12.

Marder E, Goaillard J-M (2006). Variability, compensation and homeostasis in neuron and network function. *Nat Rev Neurosci* **7**: 563–574.

Maurice N, Mercer J, Chan CS, Hernandez-Lopez S, Held J, Tkatch T *et al* (2004). D2 dopamine receptor-mediated modulation of voltage-dependent Na+ channels reduces autonomous activity in striatal cholinergic interneurons. *J Neurosci* **24**: 10289–10301.

Mermelstein PG, Song WJ, Tkatch T, Yan Z, Surmeier DJ (1998). Inwardly rectifying potassium (IRK) currents are correlated with IRK subunit expression in rat nucleus accumbens medium spiny neurons. *J Neurosci* **18**: 6650–6661.

Meshul CK, Andreassen OA, Allen C, Jørgensen HA (1996). Correlation of vacuous chewing movements with morphological changes in rats following 1-year treatment with haloperidol. *Psychopharmacology* **125**: 238–247.

Meshul CK, Casey DE (1989). Regional, reversible ultrastructural changes in rat brain with chronic neuroleptic treatment. *Brain Res* **489**: 338–346.

Mirnics K, Levitt P, Lewis DA (2006). Critical appraisal of DNA microarrays in psychiatric genomics. *Biol Psychiatry* **60**: 163–176.

Myme CIO, Sugino K, Turrigiano GG, Nelson SB (2003). The NMDA-to-AMPA ratio at synapses onto layer 2/3 pyramidal neurons is conserved across prefrontal and visual cortices. *J Neurophysiol* **90**: 771–779.

Naundorf B, Wolf F, Volgushev M (2006). Unique features of action potential initiation in cortical neurons. *Nature* **440**: 1060–1063.

Nisenbaum ES, Wilson CJ (1995). Potassium currents responsible for inward and outward rectification in rat neostriatal spiny projection neurons. *J Neurosci* **15**: 4449–4463.

Osborne PG, O'Connor WT, Beck O, Ungerstedt U (1994). Acute versus chronic haloperidol: relationship between tolerance to catalepsy and striatal and accumbens dopamine, GABA and acetylcholine release. *Brain Res* **634**: 20–30.

Peterson JD, Goldberg JA, Surmeier DJ (2012). Adenosine A2a receptor antagonists attenuate striatal adaptations following dopamine depletion. *Neurobiol Dis* **45**: 409–416.

Petreanu L, Mao T, Sternson SM, Svoboda K (2009). The subcellular organization of neocortical excitatory connections. *Nature* **457**: 1142–1145.

Plotkin JL, Day M, Peterson JD, Xie Z, Kress GJ, Rafalovich I *et al* (2014). Impaired TrkB receptor signaling underlies corticostriatal dysfunction in Huntington's disease. *Neuron* **83**: 178–188.

Plotkin JL, Shen W, Rafalovich I, Sebel LE, Day M, Chan CS *et al* (2013). Regulation of dendritic calcium release in striatal spiny projection neurons. *J Neurophysiol* **110**: 2325–2336.

Redgrave P, Rodriguez M, Smith Y, Rodriguez-Oroz MC, Lehericy S, Bergman H *et al* (2010). Goal-directed and habitual control in the basal ganglia: implications for Parkinson's disease. *Nat Rev Neurosci* **11**: 760–772.

Roberts RC, Gaither LA, Gao XM, Kashyap SM, Tamminga CA (1995). Ultrastructural correlates of haloperidol-induced oral dyskinesias in rat striatum. *Synapse* **20**: 234–243.

Seeman P, Lee T, Chau-Wong M, Wong K (1976). Antipsychotic drug doses and neuroleptic/dopamine receptors. *Nature* **261**: 717–719.

Shen W, Hamilton SE, Nathanson NM, Surmeier DJ (2005). Cholinergic suppression of KCNQ channel currents enhances excitability of striatal medium spiny neurons. *J Neurosci* **25**: 7449–7458.

Shen W, Tian X, Day M, Ulrich S, Tkatch T, Nathanson NM *et al* (2007). Cholinergic modulation of Kir2 channels selectively elevates dendritic excitability in striatopallidal neurons. *Nat Neurosci* **10**: 1458–1466.

Smith Y, Raju D, Nanda B, Pare J-F, Galvan A, Wichmann T (2009). The thalamostriatal systems: anatomical and functional organization in normal and parkinsonian states. *Brain Res Bull* **78**: 60–68.

Smith Y, Raju DV, Pare J-F, Sidibe M (2004). The thalamostriatal system: a highly specific network of the basal ganglia circuitry. *Trends Neurosci* **27**: 520–527.

Stoof JC, Kebabian JW (1982). Independent in vitro regulation by the D-2 dopamine receptor of dopamine-stimulated efflux of cyclic AMP and K+-stimulated release of acetylcholine from rat neostriatum. *Brain Res* **250**: 263–270.

Tauscher J, Jones C, Remington G, Zipursky RB, Kapur S (2002). Significant dissociation of brain and plasma kinetics with antipsychotics. *Mol Psychiatry* **7**: 317–321.

Tepper JM, Sharpe NA, Koós TZ, Trent F (1998). Postnatal development of the rat neostriatum: electrophysiological, light- and electron-microscopic studies. *Dev Neurosci* **20**: 125–145.

Turrigiano GG (2008). The self-tuning neuron: synaptic scaling of excitatory synapses. *Cell* **135**: 422–435.

Uchimura N, Cherubini E, North RA (1989). Inward rectification in rat nucleus accumbens neurons. *J Neurophysiol* **62**: 1280–1286.

Villalba RM, Smith Y (2011). Differential structural plasticity of corticostriatal and thalamostriatal axo-spinous synapses in MPTP-treated Parkinsonian monkeys. *J Comp Neurol* **519**: 989–1005.

West AR, Grace AA (2002). Opposite influences of endogenous dopamine D1 and D2 receptor activation on activity states and electrophysiological properties of striatal neurons: studies combining in vivo intracellular recordings and reverse microdialysis. *J Neurosci* **22**: 294–304.

Winton-Brown TT, Fusar-Poli P, Ungless MA, Howes OD (2014). Dopaminergic basis of salience dysregulation in psychosis. *Trends Neurosci* **37**: 85–94.

Yang Y, Calakos N (2013). Presynaptic long-term plasticity. *Front Synaptic Neurosci* **5**: 8.

Zhang W, Linden DJ (2003). The other side of the engram: experience-driven changes in neuronal intrinsic excitability. *Nat Rev Neurosci* **4**: 885–900.

Zucker RS, Regehr WG (2002). Short-term synaptic plasticity. *Annu Rev Physiol* **64**: 355–405.

Supplementary Information accompanies the paper on the Neuropsychopharmacology website (http://www.nature.com/npp)